

Leveraging Quantum Annealing for Large-Scale Household Energy Scheduling with Hydrogen Storage

Arash Khalatbarisoltani¹, Amin Mahmoudi², Jie Han³, Muhammad Saeed⁴, Wenxue Liu¹, Jinwen Li¹, Solmaz Kahourzade⁵, Amirmehdi Yazdani⁶, Xiaosong Hu¹

Abstract— Hydrogen integration into microgrids facilitates the absorption of intermittenancies from renewable energy resources. However, significant challenges remain due to complex optimization problems, particularly in large-scale applications involving multiple fuel cells (FCs) and electrolyzers (ELs) with numerous binary decision variables. This paper presents a hierarchical quantum annealing (QA) model predictive control-based power allocation framework aimed at accelerating these optimization problems. First, in a day-ahead stage, the framework determines the startup and shutdown of the FCs and ELs. The short-term stage then refines the output power of the FCs and the hydrogen generation rate of the ELs. The feasibility is evaluated through a case study consisting of multiple households in Australia. Our findings demonstrate that while the traditional optimization approach performs satisfactorily in scenarios with a small number of households, the QA approach becomes more appropriate and effectively solves the problem within an acceptable range as the number of connected households increases.

Keywords: home energy management, hydrogen grids, quantum computing, renewable energy, standalone microgrids

1. Introduction

Worldwide concerns about global warming are prompting the integration of distributed renewable energy (DRE) sources, such as solar photovoltaic panels (PVs) and wind turbines (WTs), into microgrids. Intermittency is one of the main challenges associated with DREs; consequently, conventional microgrids are evolving to incorporate multi-storage systems that enhance reliability while accommodating DREs. Each microgrid with DREs can balance power demand and supply in either interconnected or islanded modes [1]. In [2], the integration of solar PV and battery energy storage for residential houses is investigated, considering vehicle-to-home operation. Another study discusses the effects of electricity tariffs and energy sharing in grid-connected houses [3]. Islanded microgrids that utilize electrolyzers (ELs) and fuel cells (FCs) can benefit from hydrogen (H₂) as an energy vector, offering the distinct advantage of long-term storage capabilities that support a stable power supply. An additional benefit is that H₂ conversion by-products can also address the water and heating needs of connected facilities, such as residences and hospitals in islanded modes. However, the proliferation of H₂ technologies in islanded systems faces challenges due to complex optimization problems and high initial costs. In hybrid power systems (H2PS) that integrate H₂ storage, power allocation strategies (PASs) play a crucial role in enhancing performance. A PAS coordinates the operation of various components, such as PEM fuel cells (PEMFCs), ELs, batteries, and DREs, to achieve optimal power allocation under varying uncertain demands. PASs can be categorized into two types: rule-based and optimization-based. Rule-based PASs rely on predefined conditions to guide the operation of H2PS under specific scenarios. For example, a rule-based PAS is proposed in [4] for a standalone H2PS that incorporates WTs and PVs. Furthermore, [5] suggests that FC-based combined heat and power systems can significantly reduce CO₂ emissions, while the integration of FCs with supercapacitors is also discussed in [6]. Although rule-based PASs are relatively straightforward to implement, they often do not achieve optimal performance. In contrast, optimization-based PASs leverage predictive information, enabling adaptation to uncertain conditions. However, traditional optimization techniques face scalability limitations when applied to large-scale systems. The integration of FCs and ELs, due to their power constraints, necessitates high computational capacity, further exacerbating the scalability issue. Quantum computing (QC) presents a promising solution [7] and can be divided into two categories: gate-based and annealing-based. In the gate-based category, qubits are initialized in specific states, then manipulated using quantum gates to construct circuits. For example, [8] employs a Quantum Approximate Optimization Algorithm (QAOA) framework based on the Alternating Direction Method of Multipliers (ADMM) to address the unit commitment problem. Despite the benefits associated with these methods, challenges remain when applying them to power systems [9]. Conversely, quantum annealing (QA), in the second category, has demonstrated potential for effectively solving combinatorial optimization problems. For instance, [10] shows that QA outperforms QAOA in various optimization tasks. This

¹Chongqing University, Chongqing, China

²Flinders University, Adelaide, Australia

³Loughborough University, Loughborough, England

⁴Shanghai Jiao Tong University, Shanghai, China

⁵University of South Australia, Adelaide, Australia

⁶Murdoch University, Perth, Australia

study proposes a QA-based model predictive control (MPC) approach for optimal household power management with hydrogen storage, aiming to expedite the optimization solution. This approach utilizes long-term predictions to determine the status of the EL and FC after adjusting their outputs during short-term operations. The remainder of the paper is organized as follows: Section 2 presents the studied standalone households in Australia. Section 3 outlines the QA-based MPC scheduling framework. Section 4 presents the results, followed by Section 5, which summarizes the findings.

2. System model

Fig. 1 presents a multi-standalone household equipped with ELs and hydrogen storage tanks, local residential PEMFCs, and battery packs. The simulation is based on real data obtained from WTs and solar PVs. Data on load demand from one standalone household is available for only one year [11], while similar load profiles are generated for the other households. The operation of the controllable appliances is randomly distributed throughout the year [1]. The output power of each solar PV module, denoted as P_t^{PV} , is calculated as [12]

$$P_t^{PV} = \eta_p P_r^{PV} I_c (1 - 0.004(T_a - 25)) \quad (1)$$

where T_a represents the ambient temperature, I_c and P_r^{PV} represent the solar insolation and rated output power of the solar PV module, and η_p stands for the solar PV converter efficiency. The output power P_t^{WT} of a WT is considered a piecewise function of wind speed v [12]

$$P_t^{WT} = \begin{cases} 0 & v < v_c \text{ or } v > v_f \\ P_r^{WT} \left(\frac{v - v_c}{v_t - v_c} \right)^3 & v_c \leq v < v_t \\ P_r^{WT} & v_t \leq v \leq v_f \end{cases} \quad (2)$$

where $v_c = 3$ m/s, $v_t = 8$ m/s and $v_f = 22$ m/s represent the cut-in, rated and cut-out wind speeds, respectively, and P_r^{WT} denotes the rated power of the WTs.

3. Multi-stage QA-based MPC PAS framework

This study proposes a multi-stage scheduling framework to optimize the interconnected households, which integrates DRE sources with ELs and H₂ storage, as well as residential PEMFCs and local batteries, as shown in Fig. 2. The multi-stage optimization framework consists of two steps: long-term and short-term. The long-term scheduling step relies on predictions of the DERs and residential load demands. This stage primarily aims to optimize the startup and shutdown statuses of the PEMFCs and ELs for the subsequent 24-hour period using a 1-hour optimization interval, denoted by T_D . The objective function of the long-term planning step includes the costs associated with the FCs, ELs, hydrogen storage levels, and battery storage levels. The indices t and i represent the value at time t and the FC and battery of household i .

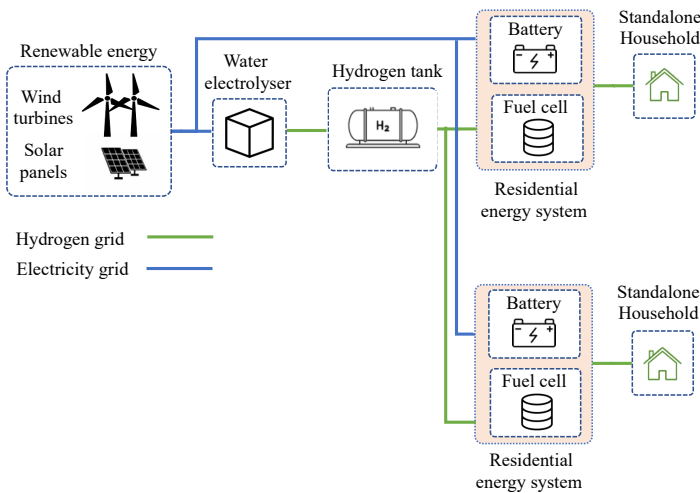


Fig. 1. Multi-standalone household integrated with hydrogen storage and renewable energy sources.

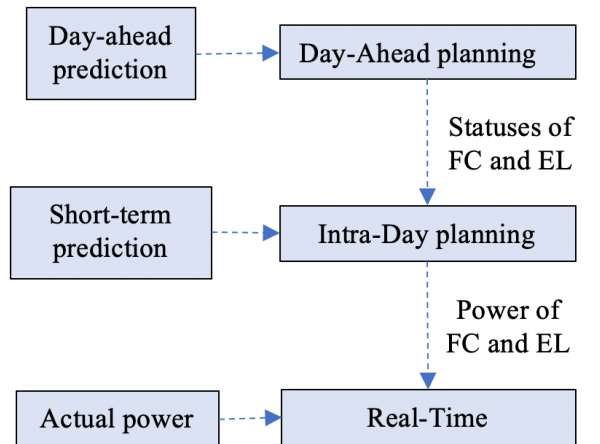


Fig. 2. The proposed multi-stage QA-based MPC PAS framework.

$$\min \sum_{i \in I} \sum_{t \in T_D} (J_{i,t}^{FC} + J_{i,t}^{EL}) - H_t + (SOC_t^{bat} - 0.7)^2 \quad (3)$$

$$U_{i,t}^{FC} + S_{i,t}^{FC} + D_{i,t}^{FC} = 1, \quad (4)$$

$$U_{i,t}^{EL} + S_{i,t}^{EL} + D_{i,t}^{EL} = 1, \quad (5)$$

$$U_{i,t}^{FC} = U_{i,t-1}^{FC} + \alpha_{i,t}^{FC} - \beta_{i,t}^{FC}, \quad (6)$$

$$U_{i,t}^{EL} = U_{i,t-1}^{EL} + \alpha_{i,t}^{EL} - \beta_{i,t}^{EL}, \quad (7)$$

$$S_{i,t}^{FC} = S_{i,t-1}^{FC} + \alpha_{s,i,t}^{FC} - \beta_{s,i,t}^{FC} - (\alpha_{i,t}^{FC} - \beta_{i,t}^{FC}), \quad (8)$$

$$S_{i,t}^{EL} = S_{i,t-1}^{EL} + \alpha_{s,i,t}^{EL} - \beta_{s,i,t}^{EL} - (\alpha_{i,t}^{EL} - \beta_{i,t}^{EL}), \quad (9)$$

$$D_{i,t}^{FC} = D_{i,t-1}^{FC} + \alpha_{s,i,t}^{FC} - \beta_{s,i,t}^{FC}, \quad (10)$$

$$D_{i,t}^{EL} = D_{i,t-1}^{EL} + \alpha_{s,i,t}^{EL} - \beta_{s,i,t}^{EL}, \quad (11)$$

$$U_{i,t+k}^{FC} \geq \alpha_{i,t}^{FC}, \quad (12)$$

$$U_{i,t+k}^{EL} \geq \alpha_{i,t}^{EL}, \quad (13)$$

$$D_{i,t+k}^{FC} \geq \beta_{i,t}^{FC}, \quad (14)$$

$$D_{i,t+k}^{EL} \geq \beta_{i,t}^{EL}, \quad (15)$$

$$P_{i,t}^{FC} \geq P_{min}^{FC} U_{i,t}^{FC}, \quad (16)$$

$$P_{i,t}^{EL} \geq P_{min}^{EL} U_{i,t}^{EL}, \quad (17)$$

$$P_{i,t}^{FC} \leq P_{max}^{FC} U_{i,t}^{FC}, \quad (18)$$

$$P_{i,t}^{EL} \leq P_{max}^{EL} U_{i,t}^{EL}, \quad (19)$$

$$SOC_{i,t}^{bat} = SOC_{i,t-1}^{bat} + \frac{\eta_c^{bat} P_{i,t-1}^{ch}}{C^{bat}} - \frac{P_{i,t-1}^{dis}}{\eta_d^{bat} C^{bat}}, \quad (20)$$

$$SOC_{i,t}^{bat} \geq SOC_{min}^{bat}, \quad (21)$$

$$SOC_{i,t}^{bat} \leq SOC_{max}^{bat}, \quad (22)$$

$$y_t^{ch} + y_t^{dis} \leq 1, \quad (23)$$

$$P_{i,t}^{ch} \leq P_{max,c}^{bat} y_t^{dis}, \quad (24)$$

$$P_{i,t}^{dis} \leq P_{max,d}^{bat} y_t^{dis}, \quad (25)$$

$$H_t = H_{t-1} + \eta^p P_{i,t}^{EL} - \eta^c P_{i,t}^{FC}, \quad (26)$$

$$H_t \geq H_{min}, \quad (27)$$

$$H_t \leq H_{max}, \quad (28)$$

$$P_t^{PV} + P_t^{WT} + P_{i,t}^{FC} + P_{i,t}^{EL} + P_{i,t}^{bat} = P_{i,t}^{load}, \quad (29)$$

where T_D denotes the set of hourly intervals across a day. The main objective function comprises costs from PEMFCs and ELs. FCs costs include standby losses and the costs of starting up and shutting down, assuming no losses when the FCs are On and Off [21]:

$$J_{i,t}^{FC} = c_s^{FC} \cdot S_{i,t}^{FC} + c_h^{FC} \cdot (\alpha_{s,i,t}^{FC} + \beta_{s,i,t}^{FC}) + c_l^{FC} \cdot (\alpha_{i,t}^{FC} + \beta_{i,t}^{FC}), \quad (30)$$

Similarly, EL costs cover the costs for standby, and both high and low transition states of ELs and are calculated:

$$J_{i,t}^{EL} = c_s^{EL} \cdot S_{i,t}^{EL} + c_h^{EL} \cdot (\alpha_{s,i,t}^{EL} + \beta_{s,i,t}^{EL}) + c_l^{EL} \cdot (\alpha_{i,t}^{EL} + \beta_{i,t}^{EL}), \quad (31)$$

where c_s^{FC} and c_s^{EL} represent the costs associated with keeping PEMFCs and ELs in standby mode, respectively. c_h^{FC} and c_h^{EL} denote the transition costs related to the startup and shutdown of PEMFCs and ELs, while c_l^{FC} and c_l^{EL} represent the transition costs associated with their operation. Equations (4) and (5) ensure that each PEMFC and EL is in exactly one state (On, Standby, or Off). The binary variables $U_{i,t}^{FC}$, $S_{i,t}^{FC}$, and $D_{i,t}^{FC}$ indicate the On, Standby, and Off statuses of the FC_i , respectively. Similarly, $U_{i,t}^{EL}$, $S_{i,t}^{EL}$, and $D_{i,t}^{EL}$ indicate the On, Standby, and Off statuses of the EL_i . Equations (6) and (7) define the state transition logic for the On status, linking it to previous states and startup/shutdown actions. Equations (4) and (5) also govern the transitions for the Standby and Off statuses for both FC_i and EL_i . These equations impose the enforced hot-start constraints, mitigating the effects of cold starts for PEMFCs and ELs. It is assumed that startup and shutdown actions cannot occur simultaneously. The minimum duration constraints in (6) and (7) enforce that units must operate for a specified minimum duration after starting up or shutting down. $T_{on,min}^{FC}$ and $T_{off,min}^{FC}$ denote the minimum number of time periods a fuel cell must remain On after startup and Off after shutdown, respectively. Similarly, $T_{on,min}^{EL}$ and $T_{off,min}^{EL}$ represent the corresponding minimum durations for the electrolyzer. Equations (16) and (19) impose the minimum and maximum power limits for PEMFCs and ELs. It is assumed that power references are static, and transient characteristics of power are not considered in this phase. $P_{i,t}^{FC}$ and $P_{i,t}^{EL}$ represent the power output of the FC_i and the power consumption of the EL_i , respectively. $P_{i,min}^{FC}$ and $P_{i,max}^{FC}$ indicate the minimum and maximum allowable output powers of the FC_i , while $P_{i,min}^{EL}$ and $P_{i,max}^{EL}$ denote the minimum and maximum allowable power consumptions of the EL_i . The battery state of charge (SOC), denoted as $SOC_{i,t}^{bat}$, is governed by Equation (20), which tracks changes in SOC over time. Equations (21) and (22) enforce the minimum and maximum SOC limits. The SOC dynamically changes based on stored energy, and charging and discharging efficiencies are represented by η_c^{bat} and η_d^{bat} , respectively, although these values may differ from one another. $P_{(i,t-1)}^{ch}$ and $P_{(i,t-1)}^{dis}$ are the power charged into and discharged from the battery at time $t - 1$, while C^{bat} is the battery capacity. SOC_{min}^{bat} and SOC_{max}^{bat} are the minimum and maximum allowable states of charge for the battery, respectively. To prevent simultaneous charging and discharging, Equation (23) is applied, while Equations (24) and (25) enforce the charging and discharging power limits. y_t^{ch} and y_t^{dis} are binary variables indicating whether the battery is charging or discharging. $P_{max,c}^{bat}$ and $P_{max,d}^{bat}$ are the maximum power limits for charging and discharging the battery. Hydrogen storage changes over time are modeled in Equation (26), with Equations (27) and (28) ensuring that the storage remains within capacity limits. The efficiencies for hydrogen production and consumption by ELs and PEMFCs are also considered as different constants. H_t represents the amount of hydrogen stored, while η^{EL} and η^{FC} are the efficiencies for hydrogen production and consumption, respectively. H_{min} and H_{max} are the minimum and maximum hydrogen storage capacities, respectively. Equation (29) enforces the power balance constraint, where P_t^{PV} is the power generated by solar PVs, P_t^{WT} is the power generated by WTs, $P_{i,t}^{FC}$ is the power output from the PEMFC, $P_{i,t}^{EL}$ is the power consumed by the EL (considered as negative generation or

load), and $P_{i,t}^{load}$ is the total electrical load demand. The short-term MPC-based stage optimizes the power outputs of the PEMFCs and ELs. The main objective is to minimize costs related to output fluctuations, denoted as C_f , while maximizing the stored H_2 and maintaining the SOC level of residential batteries, under the previous mentioned constraints.

$$\min \sum_{t \in T_{pred}} -H_{2,t}^{Str} + C_{f,t} + (SOC_t^{bat} - 0.7)^2 \quad (32)$$

$$C_{f,t} = \sum_{i \in I} \sum_{t \in T_p} (|\Delta P_t^{FC}| + |\Delta P_t^{EL}|), \quad (33)$$

where T_p denotes the 15-minute planning horizon, distinct from the 1-hour long-term scheduling period T_D considered in the previous stage. ΔP_t^{FC} and ΔP_t^{EL} represent the power changes for the PEMFCs and ELs, respectively. To implement on the QA platform, the optimization problem is formulated as a Quadratic Unconstrained Binary Optimization (QUBO) problem and then transformed into the Ising model [13]. To ensure that the transformation's accuracy loss is limited, constraints are integrated into the QUBO as penalty terms [14, 15]. The Hamiltonian of the optimization problem is constructed using the spin variables obtained from the discrete operational variables. This Hamiltonian formulation is minimized using the QA technique. The Hamiltonian formulations of all constraints and objective functions are not detailed; however, two examples are presented, and the rest follow the same analogous principles. As an example, the PEMFC state is encoded by

$$h_s^{FC} = \sum_{t \in T} \alpha_1 \left(\frac{1+f_t^W}{2} + \frac{1+f_t^V}{2} - 1 \right)^2, \quad (34)$$

where α_1 denotes the penalty coefficient, and f_t^W and f_t^V represent the spin variables related to the states of the PEMFC, respectively. Similarly, the PEMFC maximum and minimum output power constraints are applied by

$$h_p^{FC} = \sum_{t \in T} \alpha_2 \left(P_{min} \frac{1+f_t^u}{2} - \frac{1+f_t^u}{2} + s_1 \right)^2 + \alpha_3 \left(\frac{1+f_t^u}{2} - P_{max} \frac{1+f_t^u}{2} + s_2 \right)^2, \quad (35)$$

where α_2 and α_3 are penalty terms, s_1 and s_2 represent non-negative slack variables, and \bar{f}^u is the discretized and spin-transformed power output of the PEMFC.

4. Results and discussions

This section evaluates the performance of the hierarchical QA-based MPC PAS framework for multiple households with hydrogen storage, compared to the Gurobi-based approach. The QA-based implementation is achieved through D-Wave's API, which uploads the problem to a remote QA platform [13]. The values for SOC_{min} and SOC_{max} are set at 20% and 90%, respectively, with an initial SOC of 60%. Each household comprises one residential customer equipped with a 2 kW PEMFC and a 2 kW EL. The hydrogen storage tank has a capacity of 15 kg, with an initial value of 1 kg. Fig. 3 presents the results obtained from the proposed method for one household, effectively demonstrating the advantages of employing both long-term and short-term strategies. The PEMFC is utilized primarily during daytime hours when renewable energy generation is expected to meet load demands. When the battery's SOC is low, the PEMFC supplements the power load as needed. Fig. 4 illustrates the operation of the PEMFC and EL over a one-year profile using the proposed QA-based approach. At the beginning of the year, external renewable energy contributes to an increase in hydrogen storage; however, this stored hydrogen is later consumed.

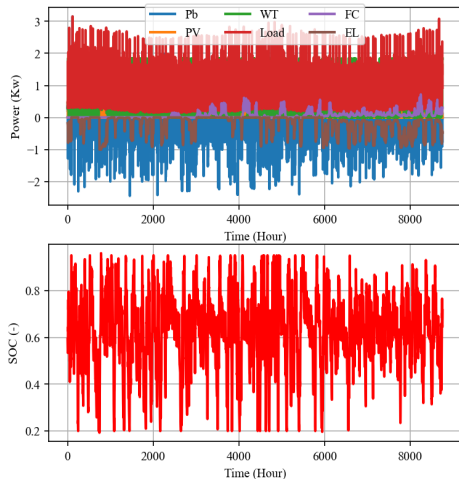


Fig. 3. a) power output profiles, b) soc SOC levels.

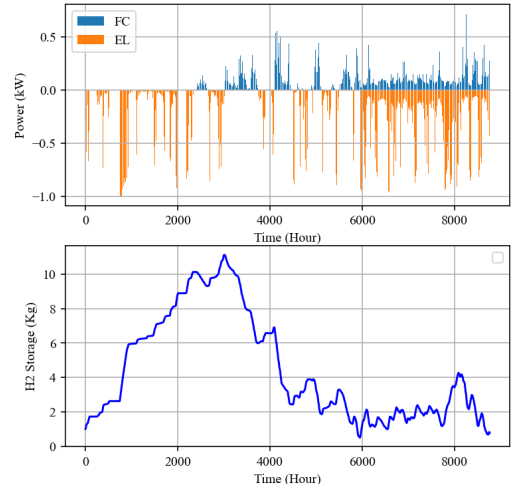


Fig. 4. a) PEMFC and EL power profiles, b) hydrogen storage.

5. Conclusion

This paper presents a hierarchical QA-based MPC framework designed for multiple households with storage capabilities. The feasibility of the proposed method was assessed using real data from a case study conducted in Australia. The approach consists of a long-term stage that determines the statuses of the PEMFCs and ELs based on projected energy demands over a one-hour horizon, as well as a short-term stage that adjusts the power outputs of the PEMFCs and ELs over a 15-minute horizon. The QA-based multi-stage strategy enhances the management of storage, preventing the depletion of low-cost resources. Our findings demonstrate that while the traditional optimization approach performs satisfactorily in scenarios with a small number of households, the QA approach becomes more suitable and effectively solves the optimization problem within an acceptable range as the number of connected households increases.

References

- [1] R. Khezri, A. Mahmoudi, and M. H. Haque, "A Demand Side Management Approach For Optimal Sizing of Standalone Renewable-Battery Systems," *IEEE Transactions on Sustainable Energy*, vol. 12, no. 4, pp. 2184-2194, 2021, doi: 10.1109/TSTE.2021.3084245.
- [2] G. Azarbaksh, A. Mahmoudi, S. Kahourzade, A. Yazdani, and A. Mahmud, "Optimal Sizing of Photovoltaic and Battery Energy Storage for Residential Houses in South Australia by Considering Vehicle-to-Home Operation," *IET Renewable Power Generation*, vol. 19, no. 1, p. e70053, 2025/01/01 2025, doi: <https://doi.org/10.1049/rpg2.70053>.
- [3] S. Khanal, R. Khezri, A. Mahmoudi, and S. Kahourzadeh, "Effects of energy sharing and electricity tariffs on optimal sizing of PV-battery systems for grid-connected houses," *Computers and Electrical Engineering*, vol. 118, p. 109457, 2024/09/01/ 2024, doi: <https://doi.org/10.1016/j.compeleceng.2024.109457>.
- [4] C. Wang and M. H. Nehrir, "Power Management of a Stand-Alone Wind/Photovoltaic/Fuel Cell Energy System," *IEEE Transactions on Energy Conversion*, vol. 23, no. 3, pp. 957-967, 2008, doi: 10.1109/TEC.2007.914200.
- [5] R. Roshandel, F. Golzar, and M. Astaneh, "Technical, economic and environmental optimization of combined heat and power systems based on solid oxide fuel cell for a greenhouse case study," *Energy Conversion and Management*, vol. 164, pp. 144-156, 2018.
- [6] D. N. Luta and A. K. Raji, "Optimal sizing of hybrid fuel cell-supercapacitor storage system for off-grid renewable applications," *Energy*, vol. 166, pp. 530-540, 2019.
- [7] E. Farhi, J. Goldstone, and S. Gutmann, "A quantum approximate optimization algorithm," *arXiv preprint arXiv:1411.4028*, 2014.
- [8] N. Nikmehr, P. Zhang, and M. A. Bragin, "Quantum distributed unit commitment: An application in microgrids," *IEEE transactions on power systems*, vol. 37, no. 5, pp. 3592-3603, 2022.
- [9] K. Blekos, D. Brand, A. Ceschini, C.-H. Chou, R.-H. Li, K. Pandya, and A. Summer, "A review on quantum approximate optimization algorithm and its variants," *Physics Reports*, vol. 1068, pp. 1-66, 2024.
- [10] E. Pelofske, A. Bärtschi, and S. Eidenbenz, "Short-depth QAOA circuits and quantum annealing on higher-order ising models," *npj Quantum Information*, vol. 10, no. 1, p. 30, 2024.
- [11] S. Khanal, R. Khezri, A. Mahmoudi, and S. Kahourzadeh, "Optimal capacity of solar photovoltaic and battery storage for grid-tied houses based on energy sharing," *IET Generation, Transmission & Distribution*, vol. 17, no. 8, pp. 1707-1722, 2023/04/01 2023, doi: <https://doi.org/10.1049/gtd2.12824>.
- [12] M. Combe, A. Mahmoudi, M. H. Haque, and R. Khezri, "Optimal sizing of an AC - coupled hybrid power system considering incentive - based demand response," *IET Generation, Transmission & Distribution*, vol. 13, no. 15, pp. 3354-3361, 2019.
- [13] N. Nikmehr, P. Zhang, H. Zheng, T.-C. Wei, G. He, and Y. A. Shamash, "Quantum annealing-infused microgrids formation: Distribution system restoration and resilience enhancement," *IEEE Transactions on Power Systems*, vol. 40, no. 1, pp. 463-475, 2024.
- [14] F. F. Silva, P. M. Carvalho, L. A. Ferreira, and Y. Omar, "A QUBO formulation for minimum loss network reconfiguration," *IEEE Transactions on Power Systems*, vol. 38, no. 5, pp. 4559-4571, 2022.
- [15] J. A. Montanez-Barrera, P. van den Heuvel, D. Willsch, and K. Michielsen, "Improving performance in combinatorial optimization problems with inequality constraints: An evaluation of the unbalanced penalization method on d-wave advantage," in *2023 IEEE International Conference on Quantum Computing and Engineering (QCE)*, 2023, vol. 1: IEEE, pp. 535-542.